WAVE DRAG DUE TO LIFT FOR TRANSONIC AIRPLANES*

Julian D. Cole
Rensselaer Polytechnic Institute

and

Norman D. Malmuth
Rockwell International Science Center

Summary

Lift dominated pointed aircraft configurations are considered in the transonic range. These are treated as lifting wings of zero thickness with aspect ratio of order one. An inner expansion which starts as Jones' theory is matched to a nonlinear outer transonic theory as in Barnwell's earlier work. New expressions for the wave drag due to the equivalent body are derived. Some examples of numerical calculations for different configurations are presented.

1. Introduction

In 1946, R. T. Jones (ref. 1) published a paper giving a formula for the lift and induced drag of "low aspect ratio pointed wings below and above the speed of sound". The work presented here, and earlier in the references cited below, represents an extension of Jones' ideas to the transonic range. It is reassuring that, under suitable circumstances, Jones' formula for the lift and induced drag not only continues to hold but is even valid for wings whose aspect ratio is order one. Under these circumstances, also shock waves and wave drag generally appear.

The basic ideas of how this type of flow behaves are set out in the report of Barnwell (ref. 2). The principal result is that the lift produces a flow that looks, in the outer region, like the flow past an equivalent axisymmetric body. This physical effect shows up in the inner and outer expansions used by Barnwell. Cheng and Hafez used similar ideas to define the apparent body and general equivalence rule in a series of papers (ref. 3, 4). Cramer (ref. 5) also studied the problem (with zero thickness as is done here) and essentially verified the results of Cheng and Hafez.

In this paper and ref. 6, we have also considered wing-like configurations with zero thickness and aspect ratio $O(1)$ as in fig. 1. Thickness effects can be incorporated relatively easily. Inner and outer expansions are defined in essentially the same manner as Barnwell although the asymptotic matching is carried out in a different way using an intermediate limit. Then wave drag associated with the outer expansion is considered. Several computations and an optimization are carried out to show the effect of planform and longitudinal distribution of lift on the transonic wave drag.

* This work was partially supported by the Air Force Office of Scientific Research under grant AFOSR 88-0037, and Rockwell North American Aircraft.

2. Basic Equations and Boundary Conditions

The problem is studied in the framework of inviscid aerodynamics. Since entropy increases across the shock waves are of third order in the flow perturbation,the full potential equation can be used as a starting point. The flow is thus, to this approximation, isentropic

$$\frac{p}{p_\infty} = \left(\frac{\rho}{\rho_\infty}\right)^\gamma \tag{2.1}$$

The potential equation is an expression of the continuity equation

$$\nabla \cdot \rho\vec{q} = 0, \quad \rho = \text{density}, \quad \vec{q} = \text{velocity} \tag{2.2}$$

Φ is the velocity potential such that $\vec{q} = \nabla\Phi$,

$$(a^2 - \Phi_x^2)\Phi_{xx} + a^2(\Phi_{yy} + \Phi_{zz}) = 2\Phi_x(\Phi_y\Phi_{xy} + \Phi_z\Phi_{xz}) + 2\Phi_y\Phi_z\Phi_{yz} + \Phi_y^2\Phi_{yy} + \Phi_z^2\Phi_{zz} \tag{2.3}$$

and a is the local speed of sound $\sqrt{\gamma p/\rho}$. The total enthalpy integral can be written

$$\frac{a^2}{U^2} = \frac{1}{M_\infty^2} + \frac{\gamma - 1}{2}\left(1 - \frac{q^2}{U^2}\right) \tag{2.4}$$

U = free stream speed, M_∞ = Mach number at infinity.

The boundary condition of flow tangent to the surface can be written

$$\nabla\Phi \cdot \nabla B = 0 \tag{2.5}$$

on $B(x, y, z) = 0$, which defines the surface.

We consider here an untwisted wing of zero thickness specified by an angle of attack α and a camber function $m(x)$. The chord of the wing $c = 1$ and the span $2b$ is $O(1)$. Thus

$$B(x, y, z) = 0 = y - \alpha f(x) + O(\alpha^3) \begin{pmatrix} 0 < x < 1 \\ -z_{LE} < z < z_{LE} \end{pmatrix} \tag{2.6}$$

where $f(x) = m(x) - x$ and $m(1) = 1$. For a straight trailing edge at $y = 0$, the trailing vortex sheet lies in the plane $y = 0, x > 1$. The planform is specified by $(\pm z_{LE}(x)), z_{LE}(1) = b$.

Another boundary condition that must be satisfied is the "Kutta condition" at a trailing edge where the flow is locally subsonic. This condition implies that the pressure loading at a trailing edge is zero. In approximations, such as the inner expansion which follows, each term satisfies this condition. Another interpretation of this condition is that unphysical pressure jumps are not allowed in the inner solutions.

3. Inner Expansion and Far Field ($r^* \to \infty$)

The approximation in general is based on $\alpha \to 0, M_\infty \to 1$ and in the usual transonic way ($K = \frac{1 - M_\infty^2}{\epsilon_1(\alpha)}$ = transonic similarity parameter, fixed). $\epsilon_1(\alpha)$ = parameter of outer expansion, defined later. In the inner expansion, the observer remains a fixed distance $O(1)$ from the wing, and distances are measured from the wing surface.

The inner limit process thus has

$$\alpha \to 0 \quad (x, y^*, z; K\text{fixed})$$

where

$$\begin{aligned} y^* &= y - \alpha f(x) \quad 0 < x < 1 \\ &= y \qquad\qquad\quad x > 1 \end{aligned} \tag{3.1}$$

The form of the inner expansion for the potential is thus

$$\Phi(x, y, z; \alpha; M_\infty) = U\{x + \alpha\varphi_1(x, y^*, z) + \alpha^2\bar{\varphi}_2(x, y^*, z) + \bar{O}(\alpha^3)\} \tag{3.2}$$

The presence of the overbar denotes the possibility of logarithmic switchback terms introduced into the inner expansion for purposes of matching with the outer expansion. Anticipating the result, we note here

$$\bar{\varphi}_2(x, y^*, z) = \log^2 \frac{1}{\sqrt{\epsilon_1}}\varphi_{22}(x) + \log \frac{1}{\sqrt{\epsilon_1}}\varphi_{21}(x) + \varphi_2(x, y^*, z) \tag{3.3}$$

Note also that the velocity components of the inner expansion are

$$\begin{aligned} \frac{q_x}{U} &= 1 + \alpha\varphi_{1x} + \alpha^2(\bar{\varphi}_{2x} - f'\varphi_{1y^*}) + \bar{O}(\alpha^3) \\ \frac{q_y}{U} &= \alpha\varphi_{1y^*} + \alpha^2\varphi_{2y^*} + \bar{O}(\alpha^3)\text{etc.} \end{aligned}$$

Substituting the assumed expansion into the full potential equation we obtain the equations for the first two approximations (in divergence forms, as follows from (2.2)) and the corresponding conditions of tangent flow

$$\nabla^{*2}\varphi_1 = 0, \qquad \varphi_{1_{y^*}}(x, 0, z) = f'(x) \begin{pmatrix} 0 < x < 1 \\ -z_{LE} < z < z_{LE} \end{pmatrix} \tag{3.4}$$

$$\nabla^{*2}\varphi_2 = \frac{\partial}{\partial x}\left\{\frac{\gamma+1}{2}\varphi_{1x}^2 + (\nabla^*\varphi_1)^2\right\}, \varphi_{2y^*}(x, 0\pm, z) = f'(x)\varphi_{1x}(x, 0\pm, z) \tag{3.5}$$

where

$$\nabla^* = \left(\frac{\partial}{\partial y^*}, \frac{\partial}{\partial z}\right) = \text{inner transverse gradient}$$

$$\nabla^*\varphi_1 = \text{inner transverse velocity perturbation}$$

$$\nabla^{*2} = \frac{\partial^2}{\partial y^{*2}} + \frac{\partial^2}{\partial z^2} = \text{inner transverse Laplacian}$$

The first equation (3.4) can be thought of as the Prandtl-Glauert equation of linearized theory but with M_∞ close to one. The second equation (3.5) shows how, in the inner representation, either compression $\varphi_{1_x} < 0$ or expansion $\varphi_{1_x} > 0$, provides an effective volume source and can cause stream tube divergence. We note the expression for the x-component of the mass flux vector.

$$\frac{\rho q_x}{\rho_\infty U} = 1 - \alpha^2 \left(\frac{(\gamma+1)}{2} \varphi_{1_x}^2 + \frac{1}{2} (\nabla^* \varphi_1)^2 \right) + \bar{O}(\alpha^3) \tag{3.6}$$

The quadratic form in (3.6) is almost the RHS of (3.5); the additional term comes from $\nabla^* \cdot (\varphi_{1_x} \nabla^* \varphi_1)$.

The inner expansion is the driver of the entire procedure. But as is now shown it is not valid as $r^* = \sqrt{y^{*2} + z^2}$ tends to infinity. On physical grounds, we would expect the transonic flow far away, which in general contains shock waves, to be described by an equation of mixed elliptic-hyperbolic type. The Laplace eqn. (3.4) is of course always elliptic.

Further, we show that the second term $\alpha^2 \varphi_2$ becomes much greater than the first $\alpha \varphi_1$ as $r^* \to \infty$. The general symmetry of the solution φ_1, φ_2 is

$$\varphi_1(x; y^*, z) = -\varphi_1(x; -y^*, z) \quad \textit{odd} \qquad \text{Lifting, vortex sheet}$$

$$\varphi_2(x; y^*, z) = \varphi_2(x; -y^* z) \qquad \textit{even} \qquad \text{Non-lifting, source}$$

We study now the behavior of these solutions near infinity in r^*. The solution for φ_1 can be represented by a dipole sheet (or vortices) or, most directly, by the use of the complex variable

$$\xi = z + i y^* = r^* e^{i(\frac{\pi}{2} - \theta^*)} \tag{3.7}$$

The complex potential for the wing, which is flat in a cross-plane $x = \text{const.}$, and for the trailing vortex sheet is

$$\begin{aligned} \varphi_1 + i\psi_1 &= -i f'(x) \left\{ \xi - \sqrt{\xi^2 - z_{LE}^2(x)} \right\} \quad 0 < x < 1 \\ &= -i f'(1) \left\{ \xi - \sqrt{\xi^2 - b^2} \right\} \qquad x > 1 \end{aligned} \tag{3.8}$$

The transverse components of velocity perturbation $\nabla^* \varphi_1 = (v_1, w_1)$ are found from

$$\begin{aligned} w_1 - i v_1 &= -i f'(x) \left\{ 1 - \frac{\xi}{\sqrt{\xi^2 - z_{LE}^2(x)}} \right\} \quad 0 < x < 1 \\ &= -i f'(1) \left\{ 1 - \frac{\xi}{\sqrt{\xi^2 - b^2}} \right\} \qquad x > 1 \end{aligned} \tag{3.9}$$

The first approximation to the pressure distribution and the lift can be found from

$$\begin{aligned} &\frac{p}{p_\infty} = \left(\frac{a^2}{a_\infty^2} \right)^{\frac{\gamma}{\gamma-1}}, \frac{a^2}{a_\infty^2} = 1 + \frac{\gamma - 1}{2} M_\infty^2 \left(1 - \frac{q^2}{U^2} \right) = 1 - \alpha(\gamma - 1) \varphi_{1_x} + \cdots \\ &\frac{p}{p_\infty} = 1 - \alpha \gamma \varphi_{1_x} + \cdots \end{aligned} \tag{3.10}$$

The dominant term is a dipole potential where the dipole strength $D_1(x)$ is equal to the lift $l_1(x)$ up to the station x. (cf 3.15)

$$\varphi_1(r^*, \theta^*; x) = \frac{l_1(x)}{2\pi} \frac{\cos\theta^*}{r^*} + O(\frac{1}{\tilde{r}^3}) \tag{3.20}$$

An unyawed symmetric planform has been assumed. For more general planforms we can use

$$D_1(x) = \int_{-z_{LE}}^{z_{LE}} [\varphi_1]_{y=0} \quad dz.$$

The potential problem for φ_2 can be thought of as describing the flow past a thin wing with thickness and a volume distribution of sources. Thus, the far field contains a source term like $\log r^*$ and a particular solution due to the RHS. From (3.20) the RHS, has a term

$$\frac{\gamma+1}{2}\varphi_{1x}^2 + \varphi_{1r^*}^2 + \frac{1}{r^{*2}}\varphi_{1\theta^*}^2 = \frac{\gamma+1}{2}(\frac{l_1'}{2\pi})^2 \frac{\cos^2\theta^*}{r^{*2}} + O(\frac{1}{r^{*4}})$$

Thus

$$\frac{\partial^2\varphi_2}{\partial r^{*2}} + \frac{1}{r^*}\frac{\partial\varphi_2}{\partial r^*} + \frac{1}{r^{*2}}\frac{\partial^2\varphi_2}{\partial\theta^{*2}} = \frac{\gamma+1}{4}\frac{\partial}{\partial x}\left\{(\frac{l_1'}{2\pi})^2\right\}\frac{1+\cos 2\theta^*}{r^{*2}} + O(\frac{1}{r^{*4}}) \tag{3.21}$$

Taking account of the particular solution, the far field of φ_2 is

$$\begin{aligned}\varphi_2(r^*, \theta^*; x) = \frac{\gamma+1}{4}\frac{l_1' l_1''}{(2\pi)^2}\log^2 r^* + S_2(x)\log r^* + g_2(x) \\ - \frac{\gamma+1}{8}\frac{l_1' l_1''}{(2\pi)^2}\cos 2\theta + \bar{O}(\frac{1}{r^{*2}})\end{aligned} \tag{3.22}$$

Thus, there is a non-uniformity as $r^* \to \infty$ (since $\alpha\varphi_1 \sim \frac{\alpha}{r^*}$, $\alpha^2\varphi_2 \sim \alpha^2 \log^2 r^*$) roughly when $r^* log^2 r^* \sim \frac{1}{\alpha}$. This shows the need for an outer expansion. An expression for the source strength $S_2(x)$ can be found from the boundary value problem for φ_2, but $g_2(x)$ is undetermined from an inner problem. $g_2(x)$ must be found by matching with the outer nonlinear boundary value problem. The presence of shock waves in the outer flow is reflected in g_2.

4. Outer Expansion and Near Field ($\tilde{r} \to 0$).

The first few terms of the outer expansion necessary to match with $\varphi_1, \bar{\varphi}_2$ are considered. The limit process associated with this expansion is the typical transonic expansion necessary to give the small disturbance equation (ref. 7). The representative point runs to infinity as $\alpha \to 0, M_\infty \to 1$. The limit process associated with this expansion has $(x, \tilde{y}, \tilde{z}, K)$ fixed as $\alpha \to 0$ where $(\tilde{y}, \tilde{z}) = \sqrt{\epsilon_1}(y, z)$.

The general form of the expansion for the potential is

$$\Phi(x,y,z;M_\infty,\alpha) = U\{x+\epsilon_1(\alpha)\phi_1(x,\tilde{y},\tilde{z};K)+\epsilon_2(\alpha)\phi_2(x,\tilde{y},\tilde{z};K)+\epsilon_3(\alpha)\phi_3(x,\tilde{y},\tilde{z};K)\cdots\} \tag{4.1}$$

where $\epsilon_1, \epsilon_2, \epsilon_3$ are found from matching. In order to match, it is necessary to obtain an RHS term similar to that in (3.5), $\frac{\gamma+1}{2}(\phi_x^2)_x$. ϕ_2 can be made to match with the dominant dipole of inner φ_1 and this forcing term then appears in the RHS of the equation for ϕ_3. ϕ_1 is a switchback type of function necessary for matching and turns out to be the axisymmetric flow produced by an equivalent body of revolution. Some details are now shown.

$$\frac{q_x}{U} = \frac{1}{U}\frac{\partial\Phi}{\partial x} = 1 + \epsilon_1\phi_{1x} + \epsilon_2\phi_{2x} + \epsilon_3\phi_{3x} + \cdots$$

$$\frac{q_y}{U} = \frac{1}{U}\frac{\partial\Phi}{\partial y} = \epsilon_1^{3/2}\phi_{1\tilde{y}} + \epsilon_2\epsilon_1^{1/2}\phi_{2\tilde{y}} + \epsilon_3\epsilon_1^{1/2}\phi_{3\tilde{y}} + \cdots \qquad etc.$$

$$\frac{a^2}{U^2} = 1 + \epsilon_1(K-(\gamma-1)\phi_{1_x}) - \epsilon_2(\gamma-1)\phi_{2x} - \epsilon_3(\gamma-1)\phi_{3x} + O(\epsilon_1^2)$$

The full potential equation (2.3) takes the form

$$\{1+\epsilon_1(K-(\gamma-1)\phi_{1x})-\epsilon_2(\gamma-1)\phi_{2x}-\epsilon_3(\gamma-1)\phi_{3x}\ldots-1-2\epsilon_1\phi_{1x}-2\epsilon_2\phi_{2x}-2\epsilon_3\phi_{3x}\ldots\}$$

$$\{\epsilon_1\phi_{1xx}+\epsilon_2\phi_{2xx}+\epsilon_3\phi_{3xx}+\ldots\}+\{1+O(\epsilon_1)\}\{\epsilon_1^2\tilde{\nabla}^2\phi_1+\epsilon_1\epsilon_2\tilde{\nabla}^2\phi_2+\epsilon_1\epsilon_3\tilde{\nabla}^2\phi_3\}$$

$$= 2\{1+\cdots\}\epsilon_1^3(\phi_{1\tilde{y}}\phi_{1x\tilde{y}}+\phi_{1\tilde{z}}\phi_{1x\tilde{z}})+\cdots$$

$$\tilde{\nabla}^2 = \frac{\partial^2}{\partial\tilde{y}^2}+\frac{\partial^2}{\partial\tilde{z}^2} \tag{4.2}$$

Thus, choosing $\epsilon_1\epsilon_3 = \epsilon_2^2$ we have

$$(K-(\gamma+1)\phi_{1x})\phi_{1xx}+\tilde{\nabla}^2\phi_1 = 0, \tag{4.3}$$

$$(K-(\gamma+1)\phi_{1x})\phi_{2xx}-(\gamma+1)\phi_{2x}\phi_{1xx}+\tilde{\nabla}^2\phi_2 = 0 \tag{4.4}$$

$$O(\epsilon_1\epsilon_3) \qquad (K-(\gamma+1)\phi_{1x})\phi_{3xx}-(\gamma+1)\phi_{3x}\phi_{1xx}+\tilde{\nabla}^2\phi_3 = (\gamma+1)\phi_{2x}\phi_{2xx} \tag{4.5}$$

ϕ_1 satisfies the usual nonlinear transonic small-disturbance (K-G) equation. ϕ_2 satisfies its linear variational equation and ϕ_3 a forced variational equation. All the equations are of conservation type and can be written

$$(K\phi_{1x}-\frac{(\gamma+1)}{2}\phi_{1x}^2)_x+\tilde{\nabla}\cdot(\tilde{\nabla}\phi_1) = 0 \tag{4.6}$$

$$(K\phi_{2x}-(\gamma+1)\phi_{1x}\phi_{2x})_x+\tilde{\nabla}\cdot(\tilde{\nabla}\phi_2) = 0 \tag{4.7}$$

$$(K\phi_{3x} - (\gamma+1)\phi_{1x}\phi_{3x})x + \tilde{\nabla}\cdot(\tilde{\nabla}\phi_3) = \frac{(\gamma+1)}{2}(\phi_{2x}^2)x \tag{4.8}$$

The near field behavior $\tilde{r} \to 0$ of these solutions, obtained from $\tilde{\nabla}^2\phi = RHS$, is given by

$$\phi_1(x_1\tilde{r}) = \mathbf{S}_1(x)\log\tilde{r} + \mathbf{G}_1(x) + 0(\tilde{r}^2\log^2\tilde{r}) \tag{4.9}$$

$$\begin{aligned}\phi_2(x_1\tilde{r},\theta) = {} & \frac{\mathbf{D}_2(x)}{2\pi}\frac{\cos\theta}{\tilde{r}} + (\gamma+1)\frac{(\mathbf{S}_1'\mathbf{D}_2')}{2\pi}\cos\theta\{\frac{1}{4}\tilde{r}\log^2\tilde{r} - \frac{1}{4}\tilde{r}\log\tilde{r} + \frac{\tilde{r}}{4}\} \\ & + \left((\gamma+1)\frac{(\mathbf{G}_1'\mathbf{D}_2')'}{2\pi} - K\frac{\mathbf{D}_2''}{2\pi}\right)\cos\theta\{\frac{\tilde{r}}{2}\log\tilde{r} - \frac{\tilde{r}}{4}) + \bar{O}(\tilde{r}^3)\end{aligned} \tag{4.10}$$

$$\begin{aligned}\phi_3(x_1,\tilde{r},\theta) + {} & \frac{(\gamma+1)}{4}\frac{\mathbf{D}_2'\mathbf{D}_2''}{(2\pi)^2}\log^2\tilde{r} + \mathbf{S}_3(x)\log\tilde{r} + \mathbf{G}_3(x) - \frac{(\gamma+1)}{8}\frac{\mathbf{D}_2'\mathbf{D}_2''}{(2\pi)^2}\cos 2\theta \\ & + \frac{(\gamma+1)^2}{16}\frac{(\mathbf{S}_1'\mathbf{D}_2'\mathbf{D}_2'')'}{(2\pi)^2}\tilde{r}^2\log^3\tilde{r} + 0(\tilde{r}^2\log^2\tilde{r})\end{aligned} \tag{4.11}$$

where $\tilde{r} = \sqrt{\tilde{y}^2+\tilde{z}^2}, \theta = \tan^{-1}\frac{\tilde{z}}{\tilde{y}} = \tan^{-1}\frac{z}{y}$
The source strength $\mathbf{S}_3$ and doublet strength $\mathbf{D}_2$ are found by matching with the inner solution. The source strength $\mathbf{S}_1$ is found in a special way in the matching. The functions $\mathbf{G}_1(x), \mathbf{G}_3(x)$ are found when the boundary value problems defined by the singular behavior as $\tilde{r} \to 0$ in (4.9, 10, 11) are solved (numerically).

5. Asymptotic Matching

A matching limit, intermediate to the inner and outer limits, is defined by a class of functions $\eta(\alpha)$ such that $\sqrt{\epsilon_1} << \eta(\alpha) << 1$. A coordinate

$$r_\eta = \eta(\alpha)r \tag{5.1}$$

is held fixed in this limit. Thus

$$r = \frac{r_\eta}{\eta} \to \infty, \qquad \tilde{r} = \frac{\sqrt{\epsilon_1}}{\eta}r_\eta \to 0$$

In the intermediate limit the representive physical radius again runs to infinity as $\alpha \to 0$, $M_\infty \to 1$ but not as fast as in the outer limit. For matching, the inner and outer limit expansions must read the same in the intermediate coordinate. Thus

$$\alpha\varphi_1 + \alpha^2\bar{\varphi}_2 + \cdots \leftrightarrow \epsilon_1\phi_1 + \epsilon_2\phi_2 + \epsilon_3\phi_3 + \cdots$$

($\leftrightarrow$ denotes "matches to")
Note that in the matching

$$\log \tilde{r} = \log \frac{\sqrt{\epsilon_1} r_\eta}{\eta} = \log \frac{r_\eta}{\eta} - \log \frac{1}{\sqrt{\epsilon_1}} \tag{5.2a}$$

and

$$\log^2 \tilde{r} = \log^2 \frac{r_\eta}{\eta} - 2 \log \frac{r_\eta}{\eta} \log \frac{1}{\sqrt{\epsilon_1}} + \log^2 \frac{1}{\sqrt{\epsilon_1}} \tag{5.2b}$$

Note also that

$$\frac{\cos\theta^*}{r^*} = \frac{y - \alpha f(x)}{y^2 + z^2 - 2\alpha y f(x)} = \frac{\cos\theta}{r} + \alpha f(x) \frac{\cos 2\theta}{r^2} + \cdots \tag{5.3}$$

Writing these out using the near field expansions of this section and the far field expansion of the previous section we have

$$\begin{aligned}
&\alpha\left(\frac{l_1 \cos\theta}{r_{\eta/\eta}} + \cdots\right) + \alpha^2 \log^2 \frac{1}{\sqrt{\epsilon_1}} \varphi_{22}(x) + \alpha^2 \log \frac{1}{\sqrt{\epsilon_1}} \varphi_{21}(x) + \alpha^2 \Big\{ \frac{(\gamma+1)}{4} \frac{l_1' l_1''}{(2\pi)^2} \log^2 \frac{r_\eta}{\eta} \\
&\qquad + S_2(x) \log \frac{r_\eta}{\eta} + g_2(x) - \frac{(\gamma+1)}{8} \frac{l_1' l_1''}{(2\pi)^2} \cos 2\theta + \bar{O}(\eta^2) \Big\} + \cdot \\
&\Leftrightarrow \epsilon_1 \left\{ \mathbf{S}_1(x)(\log \frac{r_\eta}{\eta} - \log \frac{1}{\sqrt{\epsilon_1}}) + \mathbf{G}_1(x) + \cdots \right\} + \epsilon_2 \left\{ \frac{\mathbf{D}_2(x) \cos\theta}{2\pi \sqrt{\epsilon_1} r_\eta/\eta} + \cdots \right\} + \cdot \\
&\qquad + \epsilon_3 \Big\{ \frac{(\gamma+1)}{4} \frac{\mathbf{D}_2' \mathbf{D}_2''}{(2\pi)^2} (\log^2 \frac{r_\eta}{\eta} - 2 \log \frac{r_\eta}{\eta} \log \frac{1}{\sqrt{\epsilon_1}} + \log^2 \frac{1}{\sqrt{\epsilon_1}}) + \\
&\qquad + \mathbf{S}_3(x)(\log \frac{r_\eta}{\eta} - \log \frac{1}{\sqrt{\epsilon_1}}) + \mathbf{G}_3(x) - \frac{(\gamma+1)}{8} \frac{\mathbf{D}_2' \mathbf{D}_2''}{(2\pi)^2} \cos 2\theta + \cdots \Big\}
\end{aligned} \tag{5.4}$$

Comparison of these two expansions shows that they match in an intermediate region with the choices

$$\begin{aligned}
&\frac{\epsilon_2}{\sqrt{\epsilon_1}} = \alpha && \mathbf{D}_2(x) = l_1(x) \\
&\epsilon_3 = \alpha^2, && \mathbf{S}_1(x) = \frac{(\gamma+1)}{2} \frac{\mathbf{D}_2' \mathbf{D}_2''}{(2\pi)^2} = \frac{(\gamma+1)}{2} \frac{l_1' l_1''}{(2\pi)^2} \\
&\epsilon_3 \log \frac{1}{\sqrt{\epsilon_1}} = \epsilon_1 && \mathbf{S}_3(x) = S_2(x), \mathbf{G}_3(x) = g_2(x)
\end{aligned} \tag{5.5}$$

In summary

$$\epsilon_1 = \alpha^2 \log \frac{1}{\sqrt{\epsilon_1}}, \qquad \epsilon_2 = \alpha^2 \log^{1/2} \frac{1}{\sqrt{\epsilon_1}}, \qquad \epsilon_3 = \alpha^2$$

$\epsilon_1(\alpha)$ is defined implicitly by the relationship above. $\mathbf{S}_1(x)$ is chosen by an internal switchback in the outer expansion. The switchback functions in the inner expansion are

$$\varphi_{22}(x) = -\frac{1}{2}\mathbf{S}_1(x) = -\frac{(\gamma+1)}{4}\frac{l_1' l_1''}{(2\pi)^2} \tag{5.6}$$

$$\varphi_{21}(x) = \mathbf{G}_1(x) - \mathbf{S}_3(x) = \mathbf{G}_1(x) - S_2(x) \tag{5.7}$$

The principal physical result of the matching is the source distribution for the apparent body that generates the first axisymmetric outer potential $\phi_1(x, \tilde{r})$

$$\mathbf{S}_1(x) = \frac{(\gamma+1)}{2}\frac{l_1' l_1''}{(2\pi)^2} \tag{5.8}$$

This body depends only on the longitudinal distribution of lift $l_1(x)$. A correction axisymmetric flow is provided by the source $\mathbf{S}_3$

$$\mathbf{S}_3(x) = S_2(x) \tag{5.9}$$

which generates the axisymmetric part of $\phi_3(x, \tilde{r}, \theta)$.$\phi_3(x, \tilde{r}, \theta)$ can be decomposed into

$$\phi_3(x, \tilde{r}, \theta) = \Omega_3(x, \tilde{r}) + \psi_3(x, \tilde{r}) \cos 2\theta \tag{5.10}$$

using the form of ϕ_2

$$\phi_2(x, \tilde{r}, \theta) = \psi_2(x, \tilde{r}) \cos\theta \tag{5.11}$$

Then for $\Omega_3(x, \tilde{r})$

$$(K - \gamma + 1\phi_{1x})\Omega_{3xx} - (\gamma+1)\Omega_{3x}\phi_{1xx} + \tilde{\nabla}^2\Omega_3 = \frac{(\gamma+1)}{4}(\psi_{2x}^2)_x \tag{5.12}$$

By considering the omitted terms, an overlap domain can be shown to exist for matching to this order. Also consideration of higher order terms in both expansions shows that the matching can be continued. Thus, the outer expansion reads

$$\Phi = U\{x + \alpha^2 \log\frac{1}{\sqrt{\epsilon_1}}\bar{\phi}(x, \tilde{r}, \theta) + \bar{O}(\alpha^4)\} \tag{5.13}$$

where

$$\bar{\phi} = \phi_1(x, \tilde{r}) + \frac{1}{\log^{1/2}\frac{1}{\sqrt{\epsilon_1}}}\phi_2(x, \tilde{r}, \theta) + \frac{1}{\log\frac{1}{\sqrt{\epsilon_1}}}\phi_3(x, \tilde{r}, \theta)$$

It can thus be noted that the collection of terms ϕ_1, ϕ_2, ϕ_3 which can be computed individually satisfy together the small-disturbance (K-G) equation

$$(K - (\gamma+1)\bar{\phi}_x)\bar{\phi}_{xx} + \tilde{\nabla}^2\bar{\phi} = O\left(\frac{1}{\log^{3/2}\frac{1}{\sqrt{\epsilon_1}}}\right) \tag{5.14}$$

6. Wave Drag

There is of course induced drag associated with the trailing vortex system; the drag in dominant order, associated with φ_1, is just that of Jones' theory. From the point of view of induced drag, the wing considered here, which is flat spanwise, is an optimum. The spanwise circulation distribution (cf 3.14) is elliptical. The wave drag is connected to the shock wave system in the outer flow field. It could be calculated from the entropy increase in the wave system.

For small disturbances to a free stream we have the result for the wave drag D_w

$$D_w = \rho_\infty T_\infty c^2 \int\int_{-\infty}^{\infty} [\mathbf{S}]_s dydz + \cdots \tag{6.1}$$

where $[\mathbf{S}]_s$ = jump in specific entropy across a shock. The integral is taken over all the shocks in the system. Using the expression for the entropy jump in transonic small disturbance theory (cf. ref. 7, cf. p 165 ff. for a discussion of wave drag)

$$D_w = -\rho_\infty U^2 \frac{(\gamma+1)}{12}\alpha^4 \log^2 \frac{1}{\sqrt{\epsilon_1}} c^2 \int_0^\infty \tilde{r}d\tilde{r} \int_0^{2\pi} [\bar{\phi}_x]_s^3 d\theta + \cdots \tag{6.2}$$

Consider the differential conservation form associated with (5.14)

$$\tilde{r}\left(K\frac{\bar{\phi}_x^2}{2} - \frac{(\gamma+1)}{3}\bar{\phi}_x^3 - \frac{1}{2}(\tilde{\nabla}^2\phi)^2\right)_x + (\tilde{r}\bar{\phi}_{\tilde{r}}\bar{\phi}_x)_{\tilde{r}} + \frac{1}{\tilde{r}}(\bar{\phi}_x\bar{\phi}_\theta)_\theta = 0 \tag{6.3}$$

Integrating this divergence form over all space outside a small cylinder

$$(-\infty < x < \infty) \qquad \tilde{r}_c \to 0$$

around the x-axis enables the entropy jump of (6.2) to be related to radial momentum flow. (6.3) is not conserved across shocks so that shock jumps appear such as

$$[K\frac{\bar{\phi}_x^2}{2} - \frac{(\gamma+1)}{3}\bar{\phi}_x^3 - \frac{1}{2}(\tilde{\nabla}\bar{\phi})^2]_s.$$

Let $\tilde{D}_w = \frac{Dw}{\rho_\infty U^2 c^2 \epsilon_1^2}$. Then

$$\tilde{D}_w = -\lim_{\tilde{r}_c\to 0} \tilde{r}_c \int_{-\infty}^{\infty} dx \int_0^{2\pi} d\theta \bar{\phi}_x \bar{\phi}_{\tilde{r}}|_{\tilde{r}_c} - \lim_{\substack{\tilde{r}_c\to 0,\\ x_2\to\infty}} \int_{\tilde{r}_c}^{\infty} rdr \int_0^{2\pi} d\theta \frac{(\tilde{\nabla}\bar{\phi})^2}{2}|_{x_2} \tag{6.4}$$

If we consider the dominant term in (6.4)

$$\tilde{D}_{w_1} = \int_0^1 dx \int_0^{2\pi} d\tilde{\theta} \lim_{\tilde{r}_c\to 0} (\tilde{r}_c \phi_1 \phi_{1x} \phi_{1\tilde{r}}) \tag{6.5}$$

From (4.9), $\phi_{1x} = \mathbf{S}_1'(x)\log\tilde{r} + \mathbf{G}_1'(x), \phi_{1\tilde{r}} = \frac{\mathbf{S}_1(x)}{\tilde{r}}$ and using

$$\int_0^1 \mathbf{S}_1(x)\mathbf{S}_1'(x)dx = \frac{\mathbf{S}_1^2(1)}{2} - \frac{\mathbf{S}_1^2(0)}{2} = 0$$

in which $\mathbf{S}_1(1) = \mathbf{S}_1(0) = 0$, we have

$$\tilde{D}_{w_1} = -2\pi \int_0^1 \mathbf{S}_1(x)\mathbf{G}_1'(x)dx = 2\pi \int_0^1 \mathbf{S}_1'(x)\mathbf{G}_1(x)dx \tag{6.6}$$

This drag formula is exactly that of a slender body in transonic flow (cf ref. 7, p161). Higher order terms in the drag formula can be found.

7. Applications and Remarks

Several applications have been made of the theory in its present form. For flat wings $f' = -1$. $l_1(x)$ is given by (3.15). The effective source strength for the equivalent body $\mathbf{S}_1(x) = \frac{(\gamma+1)}{2}\frac{l_1' l_1''}{(2\pi)^2}$(cf eqn. 5.5). Equation (4.3)

$$(K - (\gamma+1)\bar{\phi}_{1_x})\bar{\phi}_{1_{xx}} + \phi_{1_{\tilde{r}\tilde{r}}} + \frac{1}{\tilde{r}}\phi_{1_{\tilde{r}}} = 0 \tag{7.1}$$

is solved numerically with a small-disturbance code using (4.9) as the boundary condition for various K. The dominant term of the wave drag coefficient C_{Dw} is calculated from eqn (6.6). The results are plotted as C_{Dw} vs M_∞ for two different angles of attack in fig. 2. Substantial drag due to lift is evident. The planform shape and the distribution of $l_1(x)$ which is typical appears in fig. 3.

Another set of calculations incorporates a parabolic body of revolution (thickness ratio .057) and adds the source strength of this body to $\mathbf{S}_1(x)$. A series of planforms with semi-span $z_{LE}(x)$ given by

$$z_{LE}(x) = \frac{x(\mu - x^{\mu-1})}{\mu - 1} \tag{7.2}$$

and shown in fig. 4 was considered for various $\mu, M_\infty = .995, \alpha = .2$ rad. The idea is to optimize the L/D figure of merit $C_{Dw}/(AR = \text{aspect ratio})$ by a choice of planform. A minimum drag occurs for $\mu = 2.5$. The planform shape and curve of C_{Dw} vs. μ appears in fig. 5. Also shown in figs. (6a - 6c) for $\mu = 1.2, 2, 10$ are isobars which make evident the shock wave which occurs. The wave drag for small μ is large because of the small sweep and for large μ because of rapid changes of l_1 near the wing tip. These preliminary studies are meant to show the relative effectiveness of various planforms.

It would be very useful to extend this work to give efficient ways of calculating the higher order terms in the wave drag. It is also possible to incorporate the effects of wing thickness $\delta \sim (\alpha^2 \log \frac{1}{\sqrt{\epsilon_1}})$ into the formulation in a more systematic way. A first step in this direction is given in ref. 6.

Acknowledgement

The authors are indebted to E. Bonner of North American for valuable discussions and support.

References

1. Jones, R. T. : Properties of Low-Aspect - Ratio Pointed Wings at Speeds Below and Above the Speed of Sound. NACA Rep. 835, 1946.
2. Barnwell, R. W. : Analysis of Transonic Flow about Lifting Wing-Body Configurations. NASA TR R-440, June 1975.
3. Cheng, H. K. and Hafez, M. M. : Equivalence rule and Transonic Flow Theory Involving Lift. *AIAA J.* v. 11, No. 8, Aug. 1973, pp 1210-1212.
4. Cheng, H. K. and Hafez, M. M. : Equivalence Rule and Transonic Flows Involving Lift. USCAE Report 124, Univ. of Southern California, Apr. 1973. See also Cheng, H. K. and Hafez, M. M.: *J. Fluid Mechanics*, v. 72, 161.
5. Cramer, M. S.: Lifting Three-Dimensional Wings in Transonic Flow. J. Fluid Mech. (1979) v. 95, pp223-240. See also: A Note on 'Lifting Three-Dimensional Wings in Transonic Flow', *J. Fluid Mechanics*, (1981), v. 109, pp 257-258.
6. Malmuth, N., Wu, C. C. and Cole, J. D.: "Transonic Wave Drag - Estimation and Optimization using the Nonlinear Area Rule", *J. Aircraft* v. 24, No. 3, Mar. 1987, pp 203-210.
7. Cole, J. D. and Cook, L. P.: *Transonic Aerodynamics*, North-Holland 1986.

POINTED TRANSONIC WING

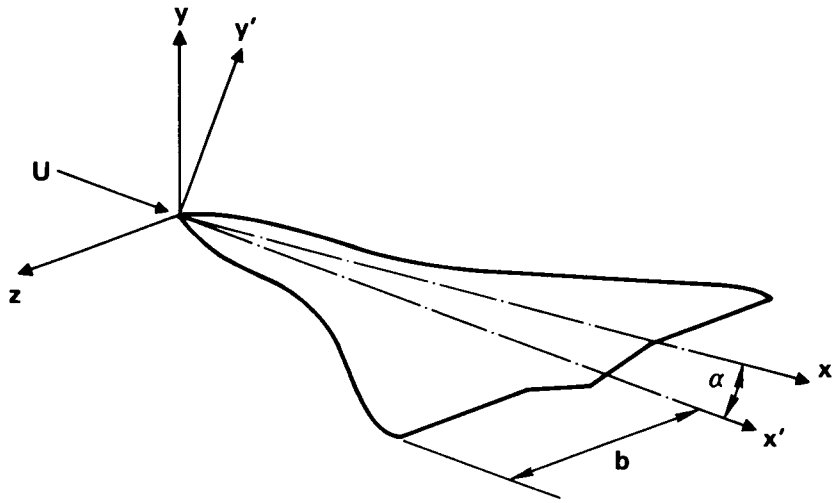

Figure 1 Pointed Transonic Wing

DRAG RISE DUE TO LIFT CHARACTERISTICS OF MODEL FIGHTER PLANFORM

100 x 50 GRID
SINE TIP FAIRING

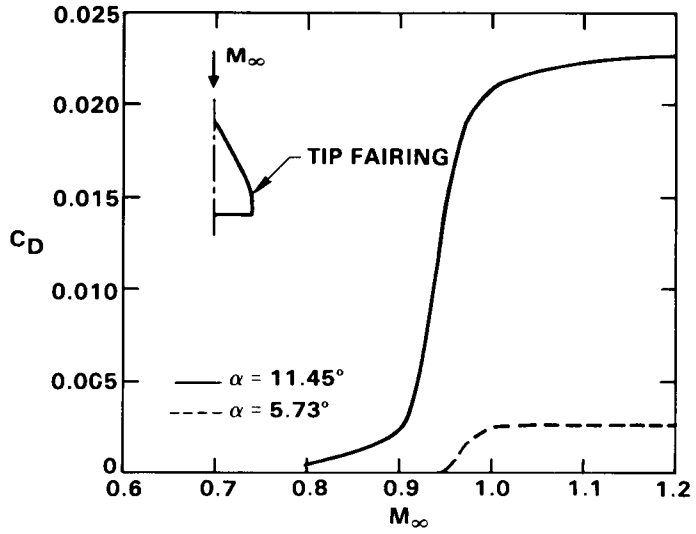

Figure 2 Drag Rise Due to Lift Characteristics of Model Fighter Planform

LIFT LOADING OF MODEL WING WITH SINE TIP FAIRING

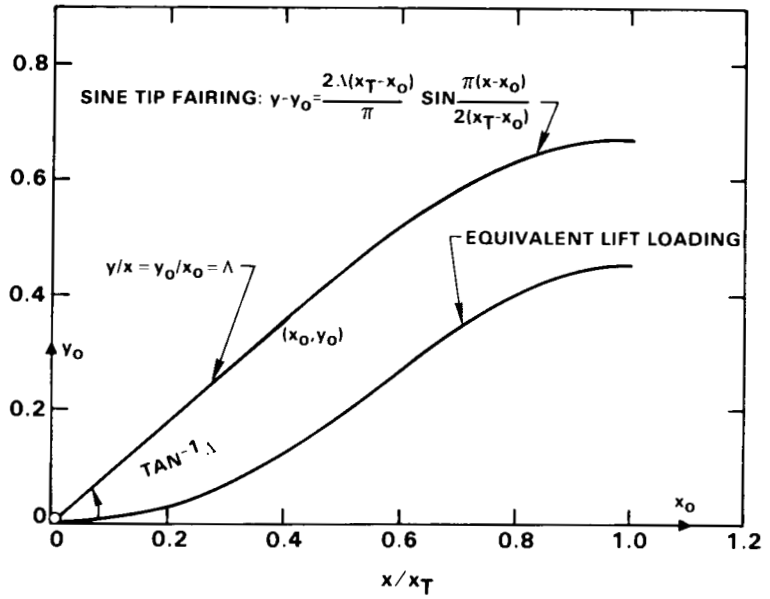

Figure 3 Lift Loading of Model Wing with Sine Tip Fairing

"μ" FAMILY OF WING BODIES IN WHICH SEMISPAN $s = \frac{\mu x - x^{\mu}}{\mu - 1}$

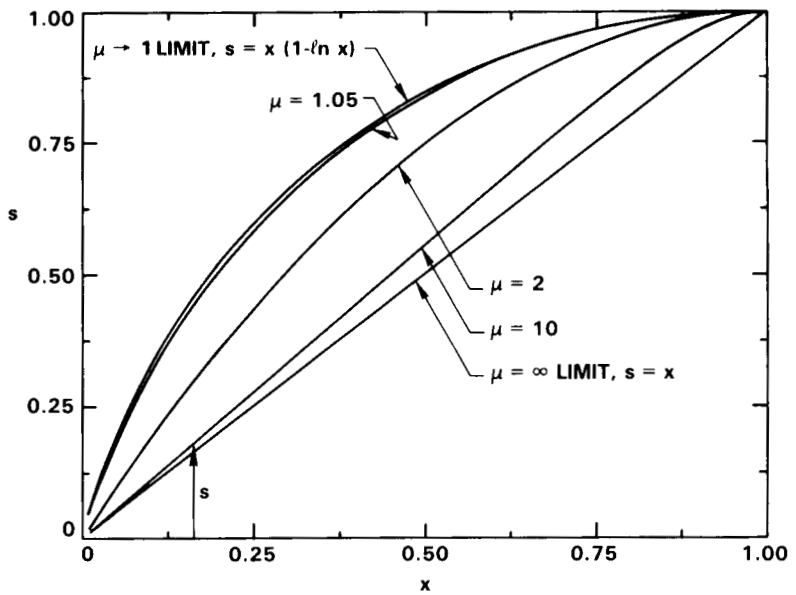

Figure 4 "μ" Family of Wing-Bodies in which Semispan = $\frac{x(\mu - x^{\mu-1})}{\mu-1}$

DRAG/ASPECT RATIO FOR μ W+B FAMILY

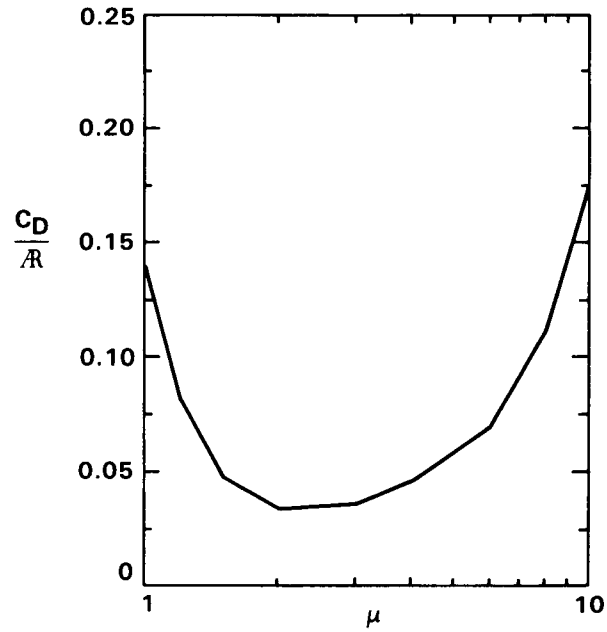

Figure 5 Wave Drag/Aspect Ratio, L/D Figure of Merit for μ Wing-Body Family, $M_\infty = .995, \alpha = .2$ rad.

ISOMACHS OF μ = 1.2 WING-BODY
M∞ = 0.995, α = 0.2 RAD., ΔM = 0.1

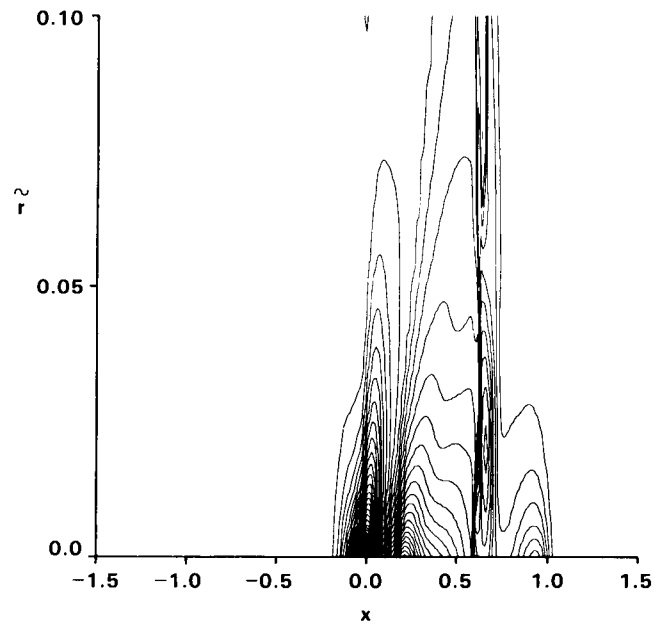

Figure 6a Isomachs of $\mu = 1.2$ Wing-Body, $M_\infty = .995$, $\alpha = .2$ rad.

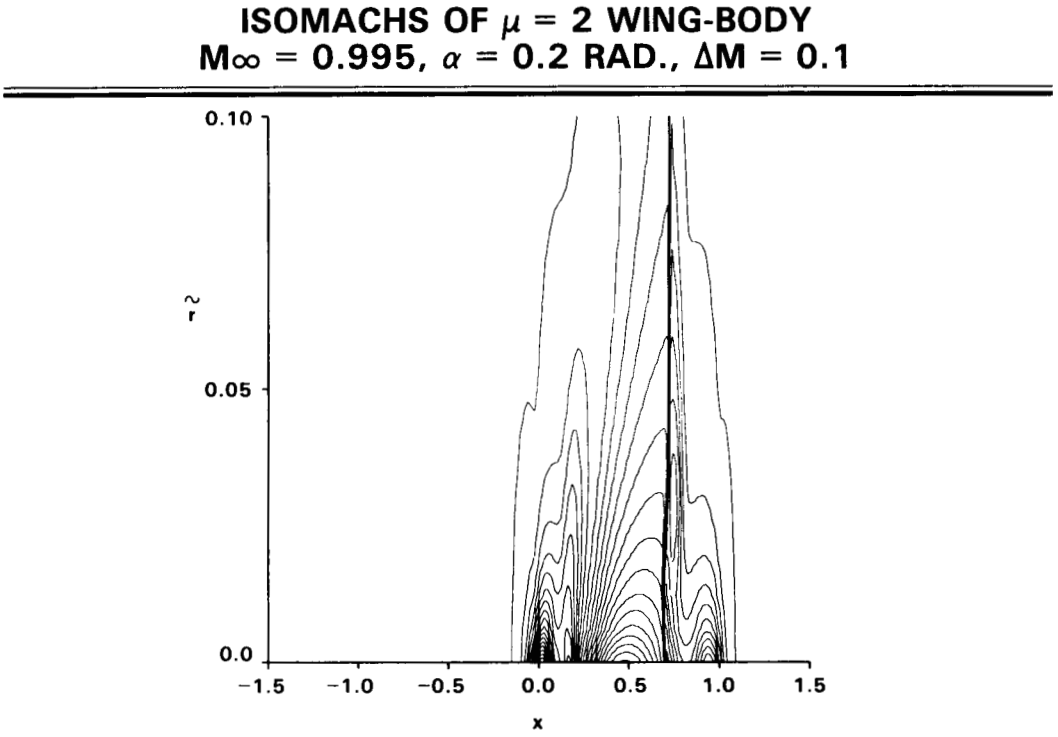

Figure 6b Isomachs of $\mu = 2.0$ Wing-Body, $M_\infty = .995$, $\alpha = .2$ rad.

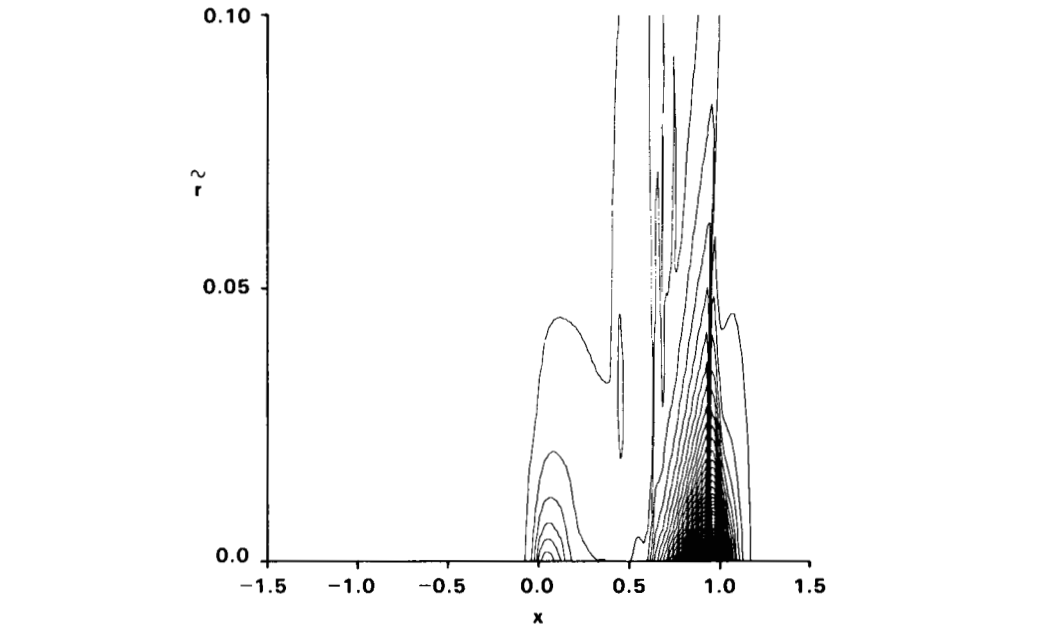

Figure 6c Isomachs of $\mu = 10.0$ Wing-Body, $M_\infty = .995$, $\alpha = .2$ rad.